Chinese Journal of Chemical Engineering 24 (2016) 1117–1121

Contents lists available at ScienceDirect

Chinese Journal of Chemical Engineering

journal homepage: www.elsevier.com/locate/CJChE

Fluid Dynamics and Transport Phenomena

Heat transfer of nanofluidics in hydrophilic pores: Insights from molecular dynamics simulations☆

Mingjie Wei, Yang Song, Yong Wang *

State Key Laboratory of Materials-Oriented Chemical Engineering, Jiangsu National Synergetic Innovation Center for Advanced Materials and College of Chemical Engineering, Nanjing Tech University, Nanjing 210009, China

ARTICLE INFO

Article history:
Received 21 October 2015
Received in revised form 20 January 2016
Accepted 28 January 2016
Available online 12 May 2016

Keywords:
Non-equilibrium molecular dynamics
Nanofluidics
Heat conduct
Temperature gradient
Fluid-wall heat transfer

ABSTRACT

Nanofluidics in hydrophilic nanopores is a common issue in many natural and industrial processes. Among all, the mass transport of nanofluidics is most concerned. Besides that, the heat transfer of a fluid flow in nano or micro channels is always considered with adding nanoparticles into the flow, so as to enhance the heat transfer by convection between the fluid and the surface. However, for some applications with around 1 nm channels such as nano filtration or erosion of rocks, there should be no nanoparticles included. Hence, it is necessary to figure out the heat transfer mechanism in the single phase nanofluidics. *Via* non-equilibrium molecular dynamics simulations, we revealed the heat transfer inside nanofluidics and the one between fluid and walls by setting simulation into extremely harsh condition. It was found that the heat was conducted by molecular motion without temperature gradient in the area of low viscous heat, while it was transferred to the walls by increasing the temperature of fluids. If the condition back to normal, it was found that the viscous heat of nanofluidics could be easily removed by the fluid-wall temperature drop of less than 1 K.

1. Introduction

Fluid flows in nanopores have attracted considerable attention for years [1], since it is related with several academic and industrial topics, such as rock erosion, ionic channel and membrane separation. For example, in the field of membrane separation, the mass transport in confinement is most concerned, so that most works are focused on fabricating new materials [2,3]. Recent findings of fast water transport in carbon-based materials [2,4–6] encourage the researchers to investigate the mechanism of mass transport of a fluid flow in nano-confinements, but it is quite difficult to study the fluid flow in nano-scale *via* direct experimental observations.

Although there are several experimental methods to observe the molecular properties of fluid, such as neutron scattering, scanning tunnel microscopy and atomic force microscopy, none of them works in the condition of a flow state. In investigating the molecular mechanism of fluid in nanopores, molecular simulations exhibit the advantage [7]. To study molecular properties of fluid at the flow state, a non-equilibrium molecular dynamics (NEMD) simulation is required, through which not only molecular properties can be calculated but also the macroscopic properties such as velocity profile and flux of the flow are obtained at the same time [8–10]. Thus there are some NEMD works published recently trying to explore why there being fast water transport in carbon nanotubes [9,11,12].

Compared to mass transport, the heat transport of nanofluidics is rarely concerned. Most researchers believe that the heat caused by viscosities (within fluid molecules) and frictions (between fluids and solid walls) is very limited as the scale of nanopores being small, so there will be hardly any heat generated in the nanofluidics. Moreover, it is generally considered that adding small particles into a fluid is one of the methods to increase the rate of heat transfer by convection between the fluid and the surface [13,14]. However, the exact cause of the enhancement of heat transfer in nanofluids is still not fully understood [15–17]. Since the concept of continuum of fluid is not applicable any more in the nano-scale, we try to find out how heat conducting in nanofluidics by NEMD simulations in this work. We build up the slit nanopores of SiO_2 and TiO_2 then let the single phase water flow through those channels *via* NEMD simulations. By analyzing the output from simulations we explore the heat conduct of nanofluidics in hydrophilic channels.

2. Simulation Details

Similar to our previous work [18,19], the slit nanopores of rutile TiO_2 and quartz SiO_2 were built as shown in Fig. 1. The area exposed to fluid molecules are 2.752×1.965 nm^2 and 2.600×2.367 nm^2 for quartz and

☆ Supported by the National Basic Research Program of China (2015CB655301), the National Natural Science Foundation of China (21506091), the Jiangsu Natural Science Foundations (BK20150944), the Special Program for Applied Research on Super Computation of the NSFC-Guangdong Joint Fund (the second phase) and the Project of Priority Academic Program Development of Jiangsu Higher Education Institutions (PAPD).
* Corresponding author.
E-mail address: yongwang@njtech.edu.cn (Y. Wang).

http://dx.doi.org/10.1016/j.cjche.2016.04.036
1004-9541/

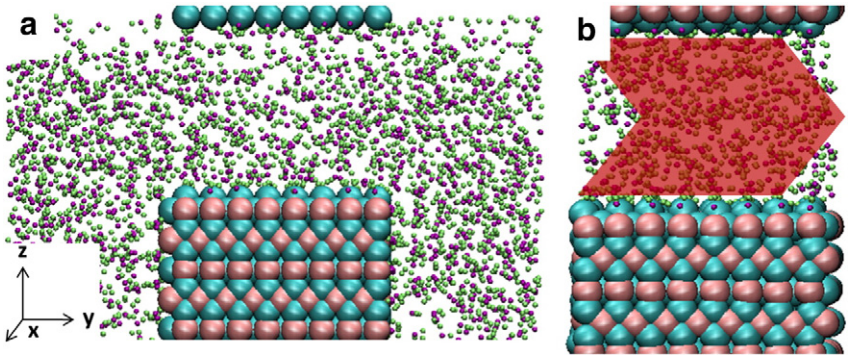

Fig. 1. Snapshot for simulation box (2.0 nm rutile slit shown only): pink, Ti; cyan, O of rutile; purple, O of water; lime, H. Red, green and blue axes represent *x*, *y* and *z* directions, respectively. (a) The initial snapshot of 1 ns NPT simulation to obtain precise water density in the slit, 3D periodical boundary condition used to form the slits. (b) The initial snapshot of 10 ns NEMD simulations with obtained water density in slits. The red arrow indicated the external force.

rutile, and the slit widths were set to be 2.0 and 2.2 nm for rutile and quartz models, respectively. SPC/E water was chosen to act as fluid in the nanopores, since SPC/E model was among the best of the non-polarizable models for water as it reproduces the vapor–liquid phase envelope as well as other structural and transport properties at ambient conditions [20,21]. The interactions of wall atoms and those between fluid and walls were described in the work of Bandura and Kubicki [22] for the rutile cases and by ClayFF [23] for quartz those.

Before a simulation of water flow in slit nanopores, the precise density of water in slits is crucial. For this reason, the isothermal-isobaric (NPT) ensemble is needed to determine the density of water in the nanopores. In order to save the computing time, only one slab of rutile or quartz was placed in each simulation box, and the slit pore could be formed by the three dimensional periodic boundary condition. If the typical three-dimensional NPT ensemble algorithm was applied in all directions, the slit width could not be preserved. To solve this problem, we applied barostat in one direction only (*y* direction in this work) while placing two water reservoirs outside the slits in *y* direction (as shown in Fig. 1a). After 1 nanosecond (ns) simulation, the average density of water in the slits was calculated. It is noted that the pressure in NPT simulations was set to 100 bars to avoid the appearance of nano bubbles.

After water molecules in the nanopores being initialized, 10 ns NEMD simulations were performed without the reservoirs (*i.e.*, restoring periodic boundary conditions in all three directions, as shown in Fig. 1b). A series of external force was added to water molecules directly to maintain the flow state [9,24,25], which are 0.2 to 1.0 in atomic unit ($kJ \cdot mol^{-1} \cdot nm^{-1}$). Some atoms in the slabs were frozen to keep the slit widths unchanged and to prevent the slab of walls from moving with the flow during simulations running and the thermostat was coupled with the other atoms of walls at 300 K. There is no thermostat directly coupled with water molecules because the thermostat will disturb the free motion of water molecules three dimensionally [26,27], so the microcanonical (NVE) ensemble was applied to water molecules [9,28]. All simulations were carried out for totally 10 ns with time step of 1.0 fs by LAMMPS package [29]. Generally, a steady state of flow reached within 100 ps, so all the data collected below came from the last 9 ns simulations for accuracy.

3. Results and Discussions

As introduced in the last section, the nanopores built in this work are slit channels, so that the velocity profile could be described, according to the theory of transport phenomenon, as [30]:

$$v_y(z) = \frac{\rho g}{2\mu}\left(l^2 - z^2\right), \tag{1}$$

where ρ and μ are the density and viscosity of fluids, respectively, and g is the gravity worked on the fluids, which came from the external force we added to each atoms in simulations. This equation is the format of Hagen–Poiseuille equation for steady flow between two parallel plates, which indicated that the velocity profile should present parabolic (shown in Fig. 2).

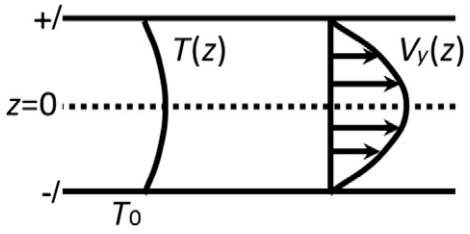

Fig. 2. The sketch of Hagen–Poiseuille equation for steady flow between two parallel plates. $T(z)$ and $V_y(z)$ are temperature and velocity profiles of fluid flows, respectively. T_0 indicates the temperature of wall atoms and the slit width is 2 *l*.

To calculate the velocity profile of water molecules, the slit channel was divided into 200 bins, then the velocities of molecules in each bin were averaged throughout 1 ns. By plotting the average velocities of each bin in one figure, we got the velocity profiles for each case (shown in Fig. 3). Actually, the velocity profile in Fig. 3 was further averaged by 9 ns (from 2 to 10 ns of each simulation) and the error bar gave the deviation of each averaged velocity from every 1 ns.

From Fig. 3, it was found that all velocity profiles of water molecules were indeed parabolic, as predicted by the Eq. (1) above. Similar results can be found in the work of simplified atom systems [31,32]. The maximum velocity was enhanced as expected while the external force increased. Moreover, in the same condition of external force, the maximum velocities of water (listed in Table 1) in quartz channel (2.2 nm wide) was higher than those in rutile channel (2.0 nm wide), which is corresponding to the prediction from HP equation as larger pore size exhibits higher velocities.

It is noticeable that the velocities of water molecules were much larger than those in natural or industrial processes. In this work, we tried to figure out how heat conducts, so we let the system generate more heat by adding much larger force on water molecules, which resulted in higher flow velocities. Although the velocities were higher than normal those, the steady state could be maintained, as the deviation of averaged velocities (error bar in Fig. 3) was small.

It is also obvious that the flow velocities of water molecules near solid walls reached zero, indicating the non-slip condition. The error bar increased in this area due to the low density of water, as fewer water molecules could be counted in to calculate the average velocities.

After the velocity profiles for each case being confirmed, the temperature profiles were then calculated, since the speed of water molecules

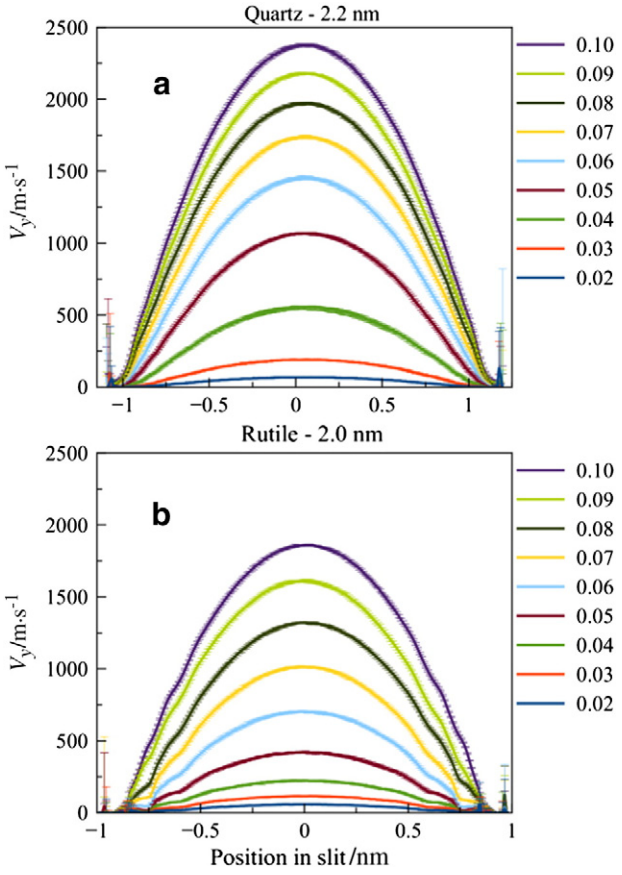

Fig. 3. Velocity profiles of water molecules for the cases of quartz (a) and rutile (b).

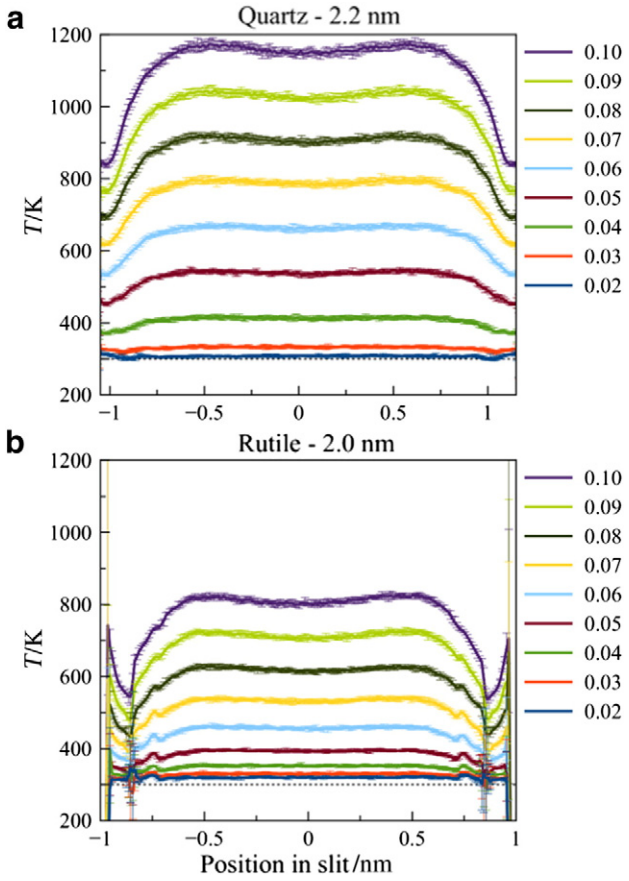

Fig. 4. Temperature profiles of water molecules for the cases of quartz (a) and rutile (b).

in flow direction (y) including the flow velocity, which should be excluded to calculate the temperature of water. The temperature profile was calculated based on the speed of each water molecules in bins as described above and the processing of averaging was the same as the one to calculate the velocity profile.

From the traditional theory of transport phenomenon, the temperature profile should be parabolic as well,

$$T(z)-T_0=\frac{\rho^2 g^2 l^4}{8k_f\mu}\left(\left(\frac{z}{l}\right)^2-1\right)^2, \tag{2}$$

where k_f is heat conductivity of water. But in Fig. 4, the temperature profiles were out of our expectation. In the central part of the slit nanopores, there were rarely temperature gradient. Outside there, the temperature of water significantly dropped, but not to the one set to the wall atoms (300 K).

Table 1
Maximum of the velocity profile in Fig. 2

External force	Maximum of velocity profile/m·s^{-1}	
	Quartz	Rutile
0.02	129.53	58.11
0.03	190.42	116.60
0.04	553.58	223.22
0.05	1067.91	420.33
0.06	1453.24	703.27
0.07	1738.47	1014.42
0.08	1972.23	1321.68
0.09	2181.60	1609.94
0.10	2376.40	1861.36

There was parabolic velocity profile for each case (shown in Fig. 3), which indicated that viscous heat was generated in the fluid including the one in central part. However, in that part, we did not find evident temperature gradient. It is most possible that the heat was conducted without temperature gradient, probably due to the molecular motion [33]. Outside the central part, there was an obvious temperature drop, which indicated that the heat conducted by only molecular motion is insufficient. Actually, the viscous heat generated in central part was small in amount due to the low velocity gradient, so the heat could easily transfer by the molecular motion. When this heat transferred outside the central part, it encountered more heat which is generated by the high velocity gradient. Hence, the accumulated heat need to be conducted by another effective way which is temperature gradient.

There was another interesting finding in Fig. 4, which was the discontinuous temperature drop between fluid and the wall, which was also found by Kim, Ali and Cagin [34]. The temperature of fluid drops dramatically near walls, but the temperature of the layer close to walls was higher than the temperature of wall atoms, probably due to the well-known Kapitza Resistance [32].

It is necessary to find out how this phenomenon occurred, and therefore we turned to the energy balance of our simulations. Once a fluid flow reaches the steady state, the viscous heat generated will be fully conducted into wall since no heat will accumulate in the system. Hence, we built up the energy balance as:

$$\frac{dW}{dt}=\frac{dQ}{dt}, \tag{3}$$

where W was the work of external forces added on water atoms equaling and Q was the heat transfer from fluid to the wall, while t

indicated the time. The work of external forces per unit time could be described as:

$$\frac{dW}{dt} = \int_{-l}^{l} V_y(z) \cdot F_{ex}\, dz. \tag{4}$$

By substituting $V_y(z)$ with Eq. (1), we could get

$$\frac{dW}{dt} = \frac{2\rho^2 g^2 l^3 L_x L_y}{3\mu}, \tag{5}$$

where L_x and L_y is the size of quartz or rutile slabs. The heat transfer was estimated by the heat transfer in solid phase, which is

$$\frac{dQ}{dt} = k_{fw} \frac{\Delta T}{D} \cdot L_x L_y, \tag{6}$$

where D indicates the distance between fluid and walls, and k_{fw} is the conductive coefficients between fluid and walls. ΔT represents $T_{fluid} - T_{wall}$.

Combining Eqs. (3), (5) to (6), we could find

$$\Delta T = \frac{2\rho^2 l^3 D}{k\mu} g^2. \tag{7}$$

From Eq. (7), there seems a linear relationship between ΔT and g^2. To make sure that linear relationship, the ΔT *vs.* g^2 was plotted (shown in Fig. 5). It is clear that all data stayed closely to the fitting line (dashed), especially for the large g cases. The probably reason for departure of data from the fitting line is the variety of k and μ, since they are dependent with the temperature of fluid.

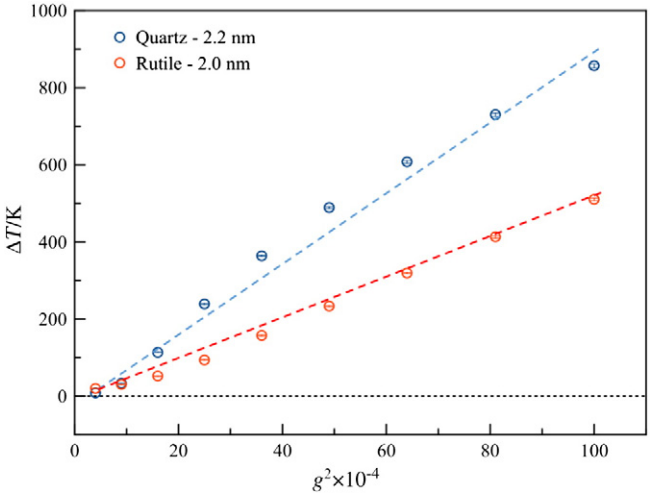

Fig. 5. The relationship between the temperature differences between fluids and walls and the square of gravity. Circles represent the data from simulations, while the dashed lines are fitting results.

The slopes of dashed lines for two kinds of walls were different, which were 9.037 and 4.956 for quartz and rutile, respectively. From Eq. (7), such difference came from not only the slit width but also the k_{fw}, the heat conductivity between fluid and walls, which is dependent of the microstructure of interfaces [35].

Although we could not easily obtain the exact relationship between ΔT and g^2, Eq. (7) disclose a fact that, for most natural and industrial processes in which g is no more than 1.0×10^{13} m · s^{-2} (equals around 30 MPa pressure drop for nanofluidics), 1 K of ΔT is sufficient to conduct heat from fluid to walls. Moreover, when the external force gets large, the fluid will rise in temperature to enhance the heat conduct between fluid and walls, so as to maintain the whole system to be steady state.

4. Conclusions

The heat transfer of nanofluidics confined in hydrophilic channels was investigated by NEMD simulations and it was found that the heat was conducted without temperature gradient in the central part of nanopores, which indicated that the heat conductivity caused by molecular thermal movement (Brownian motion) of fluids is sufficient for conducting the viscous heat in the width of around 1 nm. The heat transfer between fluids and walls was enhanced by increasing temperature of fluids itself so as to enlarge the temperature gradient between fluids and walls. However, when the fluid-wall temperature difference reached 1 K, it is efficient to transfer the heat from fluids to walls, for the lower flow velocity cases where most of the application of industries and natural processes is located. Hence, there is no need to concern the heat transfer of fluid in nanopores, especially in hydrophilic channels. It should be mentioned that the heat transfer of fluids in hydrophobic nanopores needs to be reconsidered thoroughly because the mechanism of mass transport will no longer be described by the traditional transport theories.

Nomenclature

F_{ex}	external force
g	gravity added on the fluids
k_f	heat conductivity of fluid itself
k_{fw}	heat conductivity between fluid and wall
L_x	the x length of the slab of wall
L_y	the y length of the slab of wall
l	half of the slit width ($2l$, $-l$-l)
Q	total heat transfer from fluid to wall
T	temperature of fluid
T_0	temperature of walls
ΔT	temperature drop between fluid and wall
t	time
V_y	flow velocity of water molecules in y direction
W	work of external force added onto fluid
z	position in z direction of the pores
μ	viscosity of fluid
ρ	density of fluid

References

[1] L. Bocquet, E. Charlaix, Nanofluidics, from bulk to interfaces, *Chem. Soc. Rev.* 39 (2010) 1073–1095.
[2] R. Das, M.E. Ali, S.B.A. Hamid, S. Ramakrishna, Z.Z. Chowdhury, Carbon nanotube membranes for water purification: A bright future in water desalination, *Desalination* 336 (2014) 97–109.
[3] S.P. Surwade, S.N. Smirnov, I.V. Vlassiouk, R.R. Unocic, G.M. Veith, S. Dai, S.M. Mahurin, Water desalination using nanoporous single-layer graphene, *Nat. Nanotechnol.* 10 (2015) 459–464.
[4] J.K. Holt, H.G. Park, Y. Wang, M. Stadermann, A.B. Artyukhin, C.P. Grigoropoulos, A. Noy, O. Bakajin, Fast mass transport through sub-2-nanometer carbon nanotubes, *Science* 312 (2006) 1034–1037.
[5] J. Kou, X. Zhou, H. Lu, F. Wu, J. Fan, Graphyne as the membrane for water desalination, *Nanoscale* 6 (2014) 1865–1870.
[6] D. Cohen-Tanugi, J.C. Grossman, Nanoporous graphene as a reverse osmosis membrane: Recent insights from theory and simulation, *Desalination* 366 (2015) 59–70.
[7] M. Thomas, B. Corry, T.A. Hilder, What have we learnt about the mechanisms of rapid water transport, ion rejection and selectivity in nanopores from molecular simulation? *Small* 10 (2014) 1453–1465.
[8] V.P. Sokhan, D. Nicholson, N. Quirke, Fluid flow in nanopores: Accurate boundary conditions for carbon nanotubes, *J. Chem. Phys.* 117 (2002) 8531–8539.
[9] S.K. Kannam, B.D. Todd, J.S. Hansen, P.J. Daivis, How fast does water flow in carbon nanotubes? *J. Chem. Phys.* 138 (2013) 094701.
[10] M. Whitby, N. Quirke, Fluid flow in carbon nanotubes and nanopipes, *Nat. Nanotechnol.* 2 (2007) 87–94.
[11] S. Joseph, N.R. Aluru, Why are carbon nanotubes fast transporters of water? *Nano Lett.* 8 (2008) 452–458.
[12] K. Zhao, H. Wu, Fast water thermo-pumping flow across nanotube membranes for desalination, *Nano Lett.* (2015).
[13] S. Özerinç, S. Kakaç, A. Yazıcıoğlu, Enhanced thermal conductivity of nanofluids: A state-of-the-art review, *Microfluid. Nanofluid.* 8 (2010) 145–170.
[14] J. Lv, W. Cui, M. Bai, X. Li, Molecular dynamics simulation on flow behavior of nanofluids between flat plates under shear flow condition, *Microfluid. Nanofluid.* 10 (2011) 475–480.

[15] M.M. MacDevette, T.G. Myers, B. Wetton, Boundary layer analysis and heat transfer of a nanofluid, *Microfluid. Nanofluid.* 17 (2014) 401–412.
[16] W. Cheng, R. Sadr, Induced flow field of randomly moving nanoparticles: A statistical perspective, *Microfluid. Nanofluid.* 18 (2015) 1317–1328.
[17] K. Das, Nanofluid flow over a shrinking sheet with surface slip, *Microfluid. Nanofluid.* 16 (2014) 391–401.
[18] M.-J. Wei, J. Zhou, X. Lu, Y. Zhu, W. Liu, L. Lu, L. Zhang, Diffusion of water molecules confined in slits of rutile TiO_2(110) and graphite(0001), *Fluid Phase Equilib.* 302 (2011) 316–320.
[19] M.-J. Wei, L. Zhang, L. Lu, Y. Zhu, K.E. Gubbins, X. Lu, Molecular behavior of water in TiO_2 nano-slits with varying coverages of carbon: A molecular dynamics simulation study, *Phys. Chem. Chem. Phys.* 14 (2012) 16536–16543.
[20] H.J.C. Berendsen, J.R. Grigera, T.P. Straatsma, The missing term in effective pair potentials, *J. Phys. Chem.* 91 (1987) 6269–6271.
[21] B. Guillot, Y. Guissani, How to build a better pair potential for water, *J. Chem. Phys.* 114 (2001) 6720–6733.
[22] A.V. Bandura, J.D. Kubicki, Derivation of force field parameters for TiO_2–H_2O systems from ab initio calculations, *J. Phys. Chem. B* 107 (2003) 11072–11081.
[23] R.T. Cygan, J.-J. Liang, A.G. Kalinichev, Molecular models of hydroxide, oxyhydroxide, and clay phases and the development of a general force field, *J. Phys. Chem. B* 108 (2004) 1255–1266.
[24] K.P. Travis, B.D. Todd, D.J. Evans, Poiseuille flow of molecular fluids, *Phys. A Stat. Mech. Appl.* 240 (1997) 315–327.
[25] B.D. Todd, Computer simulation of simple and complex atomistic fluids by nonequilibrium molecular dynamics techniques, *Comput. Phys. Commun.* 142 (2001) 14–21.
[26] M. Predota, P.T. Cummings, D.J. Wesolowski, Electric double layer at the rutile (110) surface. 3. Inhomogeneous viscosity and diffusivity measurement by computer simulations, *J. Phys. Chem. C* 111 (2007) 3071–3079.
[27] A. Botan, B. Rotenberg, V. Marry, P. Turq, B.T. Noetinger, "Hydrodynamics in clay nanopores", *J. Phys. Chem. C* 115 (2011) 16109–16115.
[28] V.P. Sokhan, D. Nicholson, N. Quirke, Fluid flow in nanopores: An examination of hydrodynamic boundary conditions, *J. Chem. Phys.* 115 (2001) 3878–3887.
[29] http://lammps.sandia.gov.
[30] A. Baranyai, D.J. Evans, P.J. Daivis, Isothermal shear-induced heat flow, *Phys. Rev. A* 46 (1992) 7593–7600.
[31] K.P. Travis, D.J. Evans, Molecular spin in a fluid undergoing Poiseuille flow, *Phys. Rev. E* 55 (1997) 1566–1572.
[32] B. Kim, A. Beskok, T. Cagin, Viscous heating in nanoscale shear driven liquid flows, *Microfluid. Nanofluid.* 9 (2010) 31–40.
[33] B.D. Todd, P.J. Daivis, D.J. Evans, Heat flux vector in highly inhomogeneous nonequilibrium fluids, *Phys. Rev. E* 51 (1995) 4362–4368.
[34] B. Kim, A. Beskok, T. Cagin, Thermal interactions in nanoscale fluid flow: Molecular dynamics simulations with solid–liquid interfaces, *Microfluid. Nanofluid.* 5 (2008) 551–559.
[35] X. Liang, Some effects of interface on fluid flow and heat transfer on micro- and nanoscale, *Chin. Sci. Bull.* 52 (2007) 2457–2472.